Comparison of the structural and rheological consequences of micelle formation in solutions of a model di-block copolymer

J. S. Higgins*, S. Blake*, P. E. Tomlins*, S. B. Ross-Murphy†, E. Staples‡, J. Penfold§ and J. V. Dawkins¶

**Imperial College, London SW7 2BX, UK*

†*Unilever Research, Colworth Laboratory, Sharnbrook, Beds MK44 1LQ, UK*

‡*Unilever Research, Port Sunlight Laboratory, Quarry Road East, Bebington, Wirral, Merseyside L63 3JW, UK*

§*Neutron Division, Rutherford Appleton Laboratory, Chilton, Didcot, Oxon OX11 0QX, UK*

¶*Department of Chemistry, University of Loughborough, Leics LE11 3TU, UK*

(Received 9 February 1988; revised 29 April 1988; accepted 25 May 1988)

In the selective solvent, dodecane, the di-block copolymer polystyrene-*b*-(ethylene-*co*-propylene), with a narrow molecular-weight distribution, forms micelles with polystyrene cores. Small-angle neutron scattering experiments were used to investigate both core shape and dimensions and the intercore structure factors as temperature or concentration were varied. Monodisperse spherical structures with radii around 120 Å were observed. Above a critical concentration these were arranged in relatively ordered structures in which preferred orientations could easily be induced. The core diameter and the intercore spacing were dependent on sample thermal history. During shear the intercore structure became less ordered.

The structural results correlate well with measurements of the dynamic viscosity measured in oscillatory shear, which also show a sharp change from gel-like to liquid behaviour at this critical concentration. Data are compared to model calculations in the regions where the particle form factor or where the interparticle structure factor dominate. In the latter case a hard core potential with a soft tail is found to give reasonable agreement with the data, and to allow changes with shear rate, with concentration or with temperature to be interpreted.

(Keywords: copolymer micelles; small-angle neutron scattering; rheology; scattering during shear; temperature effects; concentration effects)

INTRODUCTION

In an earlier publication[1] we described the results of small-angle neutron scattering (SANS) experiments on the model monodisperse di-block copolymer polystyrene-*b*-(ethylene-*co*-propylene) (PS–PEP) in the selective solvent, n-dodecane. This system had been shown to form micelles with very narrow size distributions[2,3]. Similar monodisperse micellar solutions have been extensively studied by X-ray scattering[4] and rheological techniques[5] and shown to form ordered structures in certain ranges of temperature and of concentration. In our work[1] we showed that the PS–PEP micelles formed by a 10 wt% solution give rise to interference scattering consistent with simple cubic structures and, moreover, that preferred orientations of these structures can easily be induced over dimensions of the order of the scattering cell (1 cm). At 2 wt% these solutions formed micelles of similar dimensions to the higher concentrations but only liquid-like interference scattering was observed.

We now investigate the effect of temperature on both the micellar dimensions and the intermicellar structures. We follow the concentration dependence of these structures between the two limits already reported and show that this concentration dependence can be correlated with rheological data obtained from the same systems.

We report observations of the changes induced in the observed intermicellar structure during shear in a Couette cell and finally we attempt an interpretation of the structure in terms of calculations based on a model potential function.

EXPERIMENTAL

Di-block copolymers

Samples of the di-block copolymer polystyrene-*b*-(ethylene-*co*-propylene) were kindly provided by Dr B Wright (Shell Research Centre, Thornton, Chester), Dr A. Bull (Shell Research BV, Amsterdam) and Ms K. F. Churchley (Shell Centre, London). The molecular weight as determined against polystyrene standards in gel permeation chromatography (g.p.c.) was $M_w = 128\,700$, $M_w/M_n = 1.06$ and the polystyrene content was 38.5 wt%. The preparations of the copolymers and of the micellar solutions have been described previously[1]. For all the SANS experiments, except those in the Couette cell, samples were syringed into flat-sided quartz cells, 1.5 × 2 cm cross section, 2 mm path length, and sealed under vacuum.

Neutron scattering experiments and analysis

Experiments were carried out using the small-angle scattering spectrometers D11 and D17[6] at the Institut

0032-3861/88/111968-11$03.00

Table 1 SANS experimental conditions

	λ (Å)	Sample–detector distance (m)	Q_{min} (Å^{-1})	Q_{max} (Å^{-1})
D11	8	10.6	5.2×10^{-3}	2.6×10^{-2}
D17	15	1.4	2.1×10^{-2}	1.05×10^{-1}

Laue–Langevin, Grenoble, France (for information, contact the scientific secretariat). The experimental conditions were as shown in *Table 1*. The scattering was corrected for background including the sample and container, and normalized for scattering geometry and detector efficiency using the incoherent scattering from water.

The shear experiments were carried out in a Couette cell which is an improved version of that described by Lindner *et al.*[7]. The main improvements are in the seals and in the drive mechanisms[8]. Shear rates up to 10^4 s^{-1} were applied to a 4 wt% micelle solution and the SANS patterns observed using the D11 spectrometer.

The normalized neutron scattered intensity per unit volume is expressed as $I(Q)$, where Q is the wavevector change on scattering, $Q=(4\pi/\lambda)\sin(\theta/2)$ (λ is the neutron wavelength, θ the scattering angle). For a particulate system the scattering depends on both the particle form factor $P(Q)$ and the interparticle interference $S(Q)$. For a system of homogeneous, monodisperse spherical particles:

$$I(Q)=KNM^2P(Q)S(Q) \tag{1}$$

where K is the contrast factor between the particles and their surroundings, and N is the number of particles per unit volume of mass M.

The contrast factor K is determined[9] by the difference in neutron scattering length density between different species. In these samples the contrast factor between the ethylene-*co*-propylene and the solvent is very small (0.39 units) compared to that between polystyrene and solvent (12.61 units) so that the SANS experiments show scattering only from the polystyrene cores and the ethylene-*co*-propylene blocks are indistinguishable from the solvent. Equation (1) may therefore be applied for the analysis of the data.

The form factor for solid spheres is[10]:

$$P(Q)=\left(\frac{3[\sin(QR)-QR\cos(QR)]}{(QR)^3}\right)^2 \tag{2}$$

The first minimum in this function occurs at $QR=4.49$.

The structure factor for particles a distance r apart is given by:

$$S(Q)=1+4\pi N\int_0^\infty [g(r)-1]\frac{\sin(Qr)}{Qr}r^2\,dr \tag{3}$$

where $g(r)$ is the radial distribution function, which is directly related to the interparticle potential[11].

At $Q=0$:

$$S(Q)\rightarrow k_BT(d\rho/d\pi) \tag{4}$$

where π is the osmotic pressure. $S(0)$ is thus determined by the osmotic compressibility of the system. A random array of hard spheres gives rise to a peak in $S(Q)$ at Q_{max} such that:

$$Q_{max}d=2\pi\alpha \tag{5}$$

where d is the mean interparticle spacing and α is a constant close to unity. For close packing[12] $\alpha=1.22$ whereas Pusey[13] has shown that for liquid-like structures $\alpha=1.18$. For low particle density, and also as Q increases, $S(Q)\rightarrow 0$. We thus have in equation (1):

$$P(Q)\rightarrow 1 \quad \text{for } Q<4.5R^{-1} \tag{6a}$$

$$S(Q)\rightarrow 1 \quad \text{for } Q>2\pi d \tag{6b}$$

and since the minimum value of $d=2R$:

$$S(Q)\rightarrow 1 \quad \text{for } Q>4\pi R^{-2} \tag{6c}$$

The effect of these limits is that for reasonably dilute solutions where $d\gg 2R$ the scattering from $P(Q)$ and from $S(Q)$ are effectively seen separately in the scattering patterns. This is the case for all the data reported here.

Viscoelastic measurements

Rheological measurements in shear were performed using a Rheometrics Mechanical Spectrometer (RMS 605M) using cone-and-plate geometry. Both steady and oscillatory shear measurements were performed at 25°C, using 2.5 cm diameter (cone angle 0.1 rad) and 1.25 cm (0.04 rad) cones—the larger radius cone being employed for the lower concentration samples to generate more torque.

At the edge of the cone-and-plate fixture where there would be an air interface the solution was protected by a light silicone oil. Strain sweeps (strain increased from 0.01 to 1) were performed at three different oscillatory frequencies (1.0, 10.0 and 100.0 rad s^{-1}) to establish the linear viscoelastic strain limit, and then frequency sweeps were performed over the range 0.01 to 100 rad s^{-1}. Steady shear measurements were also performed for shear rates from 0.01 up to a maximum of 10^3 s^{-1}. For the most concentrated solutions the torque generated at the higher shear rates became too great for the transducer system.

Measurements of the recovery of the stress overshoot ratio were also performed. The sample was subjected to a steady shear rate of 5 s^{-1} for 10 s (i.e. 50 strain units)—judged sufficient to destroy any 'history' induced by loading, etc., and allowed to recover for time t ($t=5$–10^4 s) before remeasuring the start stress–time profile at $\dot\gamma=5$ s^{-1}. The peak stress σ_{max} and long-time steady stress σ_{ss} were noted and the overshoot ratio σ_{max}/σ_{ss} was charted against recovery time t. For experiments at long times the internal triangular wave generator of the RMS was employed. This technique has recently been shown to be more reliable for long-time 'start-shear' experiments[14].

RESULTS AND DISCUSSION

Effects of temperature and implications for sample preparation

In *Figure 1* the observed particle form factors for a 6% solution before, during and after heating to 160°C are compared. The full curves through the data points are the best fits of equation (2) with a Gaussian spread of values for the radii. Best-fit radii and standard deviations are listed in *Table 2*. It can be seen that the scattering signal characteristic of the micelle cores (equation (2)) all but disappears at the highest temperature and that the minimum moves to higher Q indicating that the micelle radius is reduced as temperature is raised, and remains at a smaller value on cooling. Similar reductions in core

dimensions were observed on heating 8% and 10% solutions as seen in *Table 2*. The sample preparation technique involves dissolving the copolymer in methylene chloride before adding dodecane to form micelles. The methylene chloride is then removed by heating to 70°C. Samples loaded into sealed cells were also heated to around 70°C to facilitate flow of the viscous solutions. It is thus clear that differences in core dimensions may vary from sample to sample depending on the exact treatment undergone. It was noted for example that samples not preloaded into the sealed cells always had dimensions about 20% smaller than those in the cells.

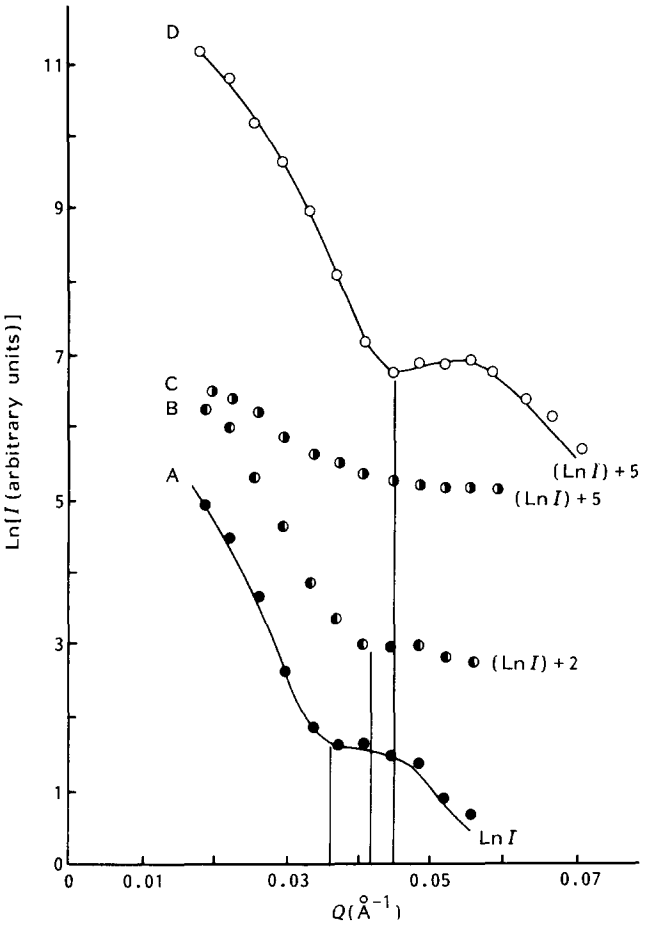

Figure 1 Ln $I(Q)$ vs. Q at high Q where $P(Q)$ dominates scattering for a 6% sample before, during and after heating to 160°C: A, before; B, 110°C; C, 160°C; D, after. The full curves are the best fits of equation (1) with values of R and the spread in R as given in *Table 2*

The reduction in core dimensions is accompanied by a corresponding decrease in the interparticle spacing. *Figure 2* shows this effect as an 8% sample is heated to 130°C. The d-spacings are listed in *Table 2*.

It was observed previously that in the higher-concentration samples anisotropy of the scattering patterns was apparently introduced. Such non-random orientation is seen for this 8% sample in the two-dimensional intensity maps in *Figure 3*. Moreover, the actual orientation is preserved through the heating cycle while the particle dimensions and interparticle spacings reduce in magnitude. For this 8% sample (and for other high-concentration samples) three peaks are observed in the $S(Q)$ data, and the corresponding d-spacings ($d=2\pi/Q_{max}$) are listed in *Table 2*. In our previous publication[1] we showed that for a 10% sample the positions of the three peaks were consistent with either a simple cubic or a body-centred cubic structure.

The d-spacings are given by:

$$d_{hkl}=a_0h^2+k^2+l^2)^{-1/2} \quad (7)$$

where h, k, l are the Miller indices and a_0 is the unit-cell dimension. For both simple cubic and body-centred cubic structures the ratio of the first three layer lines expressed as d_1^2/d_n^2 are 1:2:3. *Table 2* shows that the current samples show d-spacings with approximately these relative values. In order to distinguish between the two cubic structures, therefore, we took into account the observed core radii and known concentrations. The micelle number density can be calculated in two ways. For a core radius R, and assuming a density of PS of approximately 1.0 g cm^{-3}, the weight of polystyrene in each micelle is given by $4/3\pi R^3\rho$.

Table 2 SANS dimensions

w (wt%)	Conditions (assumed RT/sealed cells unless specified)	R(st. dev.) (Å)	d ($=2\pi/Q_{max}$) (Å)	
2		–	966	Isotropic
3		150 (28)	1047	Isotropic
4		–	1083	Isotropic
4	In free loaded cell	96 (10)	–	
4	In Couette cell	–	604^1, $410^{2.1}$, 348^3	Barely anisotropic
5		130 (42)	728, 418	Isotropic
6	Before heating	110 (19)	665, 390	Barely anisotropic
6	110°C	110 (17)	–	
6	After heating to 160°C	100 (14)	523^1, $359^{2.1}$, $314^{2.7}$	Isotropic
7		–	644^1, $434^{2.2}$, 369^3	Anisotropic
8	Before heating	127 (16)	621^1, $419^{2.1}$, 355^3	Anisotropic
8	100°C heating	–	573^1, 405^2, 329^3	Anisotropic
8	130°C	–	481^1, 339^2, 279^3	Anisotropic
8	100°C cooling	–	487^1, 339^2, 284^3	Anisotropic
8	73°C	–	493^1, $343^{2.1}$, 287^3	Anisotropic
8	After heating	92 (13)	–	
8	In free loaded cell	104 (12)	–	
8	In Couette cell	–	560, 345	Isotropic
9	After heating	100 (±25)	473^1, $326^{2.1}$, 276^3	Barely anisotropic
10	Before heating	130 (17)	–	
10	After heating	107 (16)	471^1, $327^{2.1}$, 274^3	Barely anisotropic

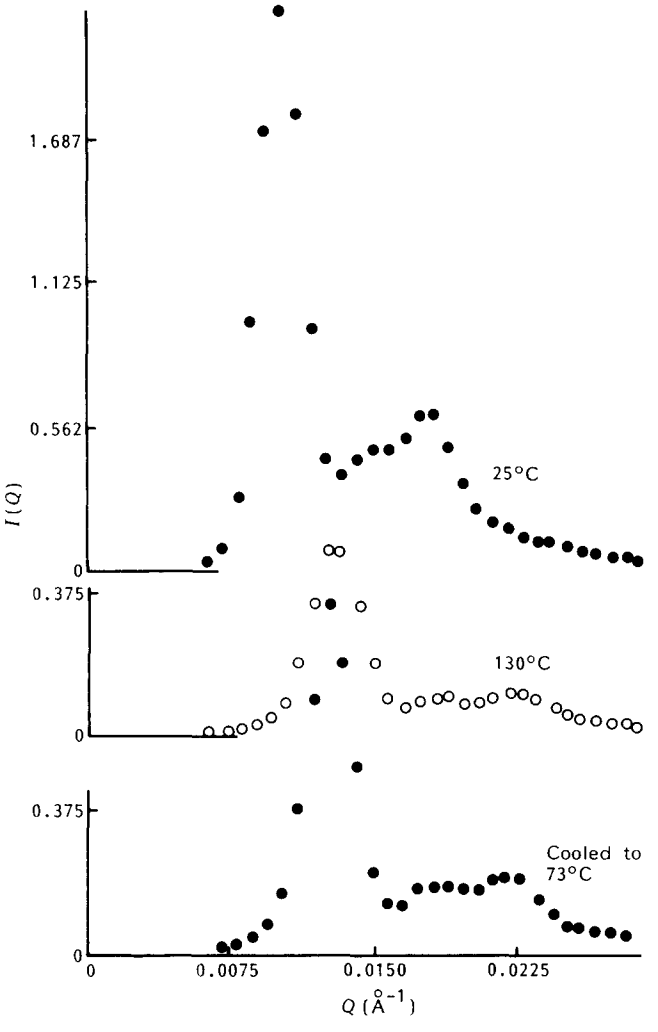

Figure 2 $I(Q)$ vs. Q at low Q where $S(Q)$ dominates the scattering for an 8% sample before and during heating to 130°C and subsequent cooling

Using the weight per cent values w given in *Table 2* the number of particles per unit volume is given by:

$$N = \frac{3}{4\pi}\frac{0.38w}{\rho R^3} \tag{8}$$

This assumes that *all* material is included in micelles. This seems reasonable because the critical micelle concentration at 84°C in n-decane (a better solvent than dodecane) is less than 0.0004%[3] and for higher alkanes solubility reduces still further. Alternatively, if the core particles are arranged on a regular lattice of dimension a_0 then the number of particles per unit volume $N' = a_0^{-3}$ for a simple cubic structure or $2(a_0)^{-3}$ for body-centred with two lattice points per unit cell. For simple cubic structure $a_0 \equiv d$ but for body-centred structures $a_0 = (\sqrt{2})d$. In *Table 3* we compare values of N and of N' for samples for which d_1 and R are available.

It is seen that generally the values of N lie between the value of N' for the body-centred cubic structure and the simple cubic structure. It is important to comment therefore on our earlier work where we observed apparently good agreement with simple cubic structures for N and N'. A small error in the calculation of the concentration in that paper means that the sample with 10% concentration actually contained 0.09 g ml^{-1}. The mass of PS per cubic centimetre is thus 0.0346 cm^{-3} and then also the distinction between b.c.c. and s.c. can no longer be so clearly made, N falling between the values of N' for the two structures. Given the preservation of preferred orientation while micelles become smaller and closer together (difficult to imagine in a three-dimensional array), this inexactness in the structural analysis may indicate layered structures of some type. In any case these temperature measurements underline the sensitivity of the micelle dimensions and organization to the exact preparative procedure employed, and to the subsequent handling of samples. It should be noted that if the PS cores were diluted with solvent (either residual methylene chloride or n-dodecane) then N in *Table 3* would be increased towards N'_{sc}. Information on the glass transition temperature of the PS in the cores would provide information on its level of plasticization and hence the presence of solvent. T_g data are not available for our samples, but Candau *et al*[15] investigated the n.m.r. spectra of a similar copolymer in a series of n-alkanes. For n-dodecane some level of plasticization was observed due to its effect on segment mobility and we thus have to assume that our values of N in *Table 3* will move towards N'_{sc}. For n-dodecane these authors observed a high level of micelle dissociation above 100°C with complete dissociation at around 150°C. This is in good agreement with our own observation that the PS cores change dimensions and dissociate at high temperature. It is also in agreement with the reduction in intensity observed at high temperatures and its subsequent recovery at lower temperatures in *Figures 1* and *2*. The existence of free copolymer in the solvent will greatly reduce the contrast factor K in equation (1).

In a recent paper[16] Mortensen *et al.* have observed SANS from low concentrations of these micelles. They observed radii around 100 Å for the PS cores and a reduction at elevated temperatures. This reduction was reversible, however. Discussion with these authors revealed that their samples had already been heated once to dissociation before the measurements reported. It thus appears likely that in our heated runs a new equilibrium radius is reached and that in subsequent high-temperature experiments a further reversible decrease in R might also be observed. If we assume a density of 1 g cm^{-3} for the polystyrene cores, the surface area per molecule can be calculated from the volume per polystyrene segment V_m, and the number of molecules per micelle ($=4\pi R^3/3V_m$). Thus the surface area per molecule is $S = 3V_m/R$. In *Table 3* these values are listed in the final column and it is interesting to note that there is a tendency to increase S after heating towards a fairly constant value of around 2.4×10^3 Å^3. This suggests that equilibrium may be determined by the surface area required per molecule.

Effects of concentrations on rheology and interparticle structure

Figure 4 shows the frequency dependence of the dynamic viscosity η^* ($=G^*/\omega$) for samples with concentrations 2.46 to 10% w/w. For those with nominal concentrations of 2.46, 2.75 and 3%, the response is almost completely Newtonian, with only a slight indication of pseudoplasticity ('shear thinning') at the highest frequency[17]. For these samples, the shear-rate dependence of steady shear viscosity (η measured for

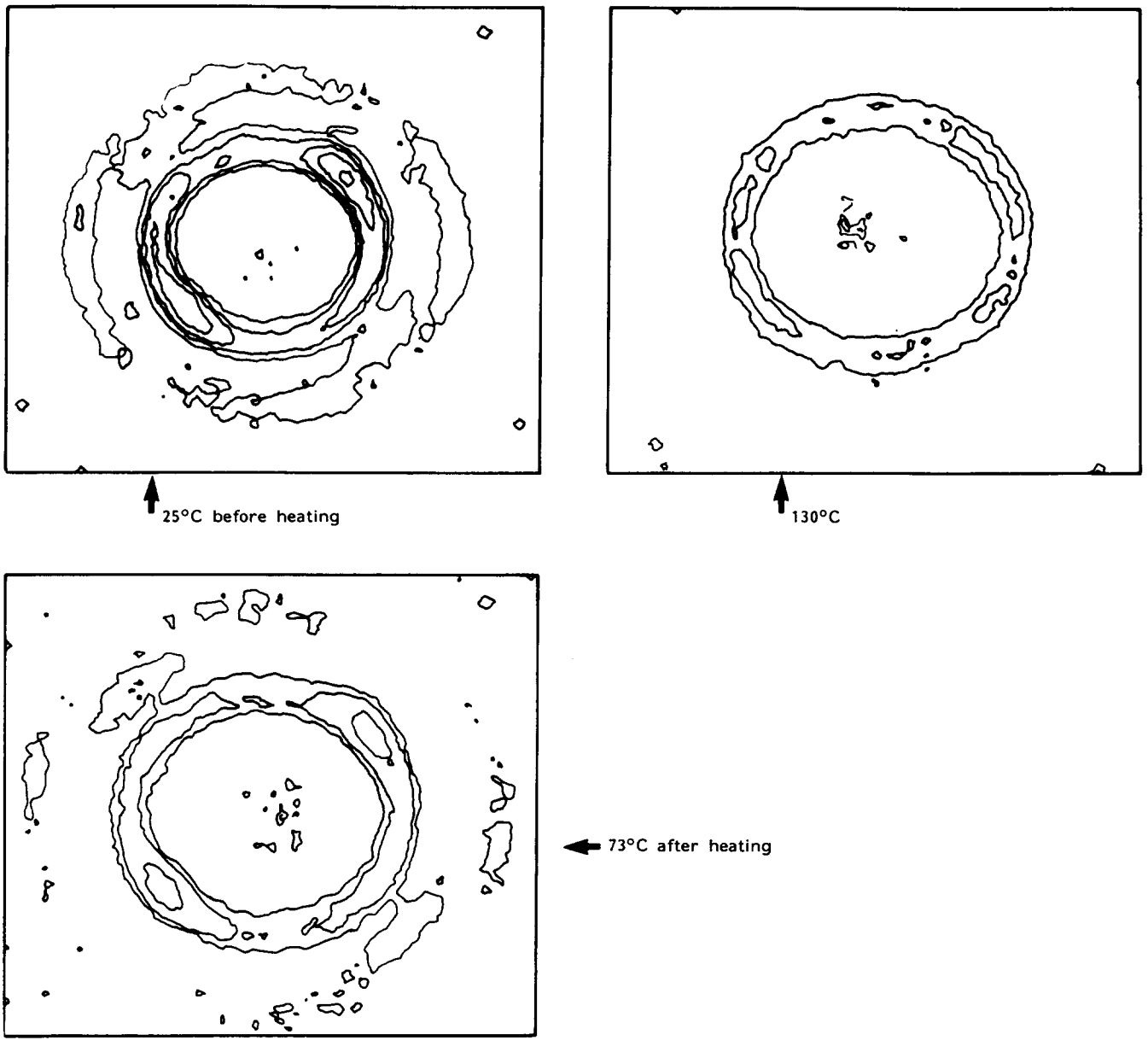

Figure 3 Two-dimensional intensity maps for the same data as shown in *Figure 2*

Table 3

w (wt%)	Conditions	W_{ps}	R (Å)	d_1 (Å)	N (cm^{-3})	N'_{sc} (cm^{-3})	N'_{bcc} (cm^{-3})	S/molecule (Å)
5		0.019	130	728	2.06×10^{15}	1.85×10^{15}	1.85×10^{15}	1.9×10^{3}
6	Before heating[a]	0.023	110	665	4.12×10^{15}	3.40×10^{15}	2.41×10^{15}	2.2×10^{3}
6	After heating	0.023	100	523	5.49×10^{15}	6.99×10^{15}	4.94×10^{15}	2.4×10^{3}
8	Before heating	0.030	127	621	3.49×10^{15}	4.18×10^{15}	2.95×10^{15}	1.9×10^{3}
8	After heating	0.030	92	493	9.20×10^{15}	8.34×10^{15}	5.91×10^{15}	2.6×10^{3}
9	After heating[a]	0.034	103	473	7.42×10^{15}	9.45×10^{15}	6.70×10^{15}	2.4×10^{3}
10	After heating	0.038	107	471	7.40×10^{15}	9.57×10^{15}	6.78×10^{15}	2.3×10^{3}

Notes
(1) If ρ for PS cores is $<\rho_{PS}$ (re. methylene chloride trapped), then N *increases* $\rightarrow N'_{sc}$
(2) This calculation takes no account of polydispersity in R
(3) Or of the surface profile of the spheres
[a] For 6% before heating there was a broad distribution in R which may account for $N > N'_{sc}$ while for 9% we could not achieve a good fit for $P(Q)$

different $\dot{\gamma}$) and the dynamic viscosity measured for different ω were almost completely superposable—the Cox–Merz[15] rule was obeyed.

For the other samples, η^* has very pronounced frequency dependence (and η depends strongly on $\dot{\gamma}$), and further $\eta^*(\omega)$ profiles lie above $\eta(\dot{\gamma})$—there is no Cox–Merz superposition. Both properties are typical of structured fluids—the so-called 'weak gels'[14]. The inset to *Figure 4* charts the concentration dependence of the dynamic viscosity of these systems at 1.0 rad s^{-1}. Apart

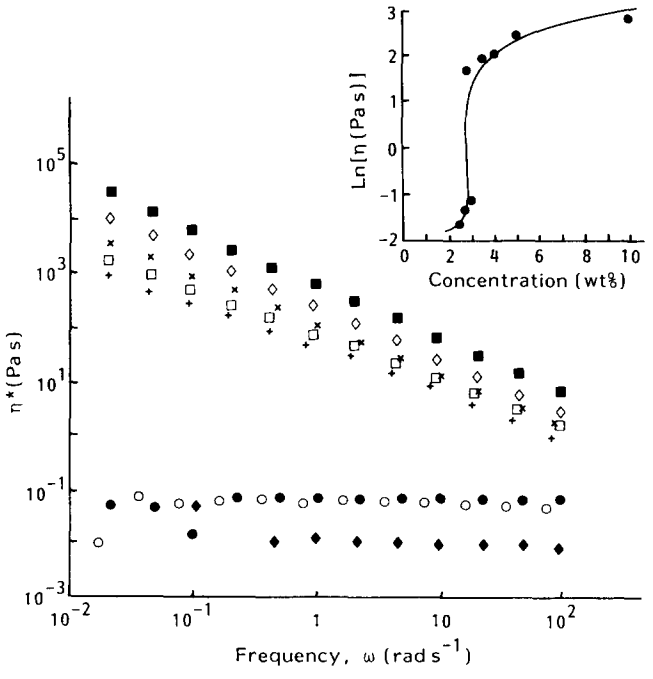

Figure 4 Frequency dependence of dynamic viscosity (η^*) for a range of different concentrations in dodecane. Inset: the concentration dependence of η^* at 1 rad s^{-1}. Concentrations: ◆, 2.4%; ○, 2.75%; ●, 3%; +, 2.84%; □, 3.5%; ×, 4%; ◇, 5%; ■, 10%

from the anomalous behaviour of the sample prepared at 2.84% w/w, there is a clear transition from the non-structured to a structured system occurring at ≃3% w/w concentration. This anomalous sample illustrates both the criticality of the transition and the consequent sensitivity to slight variations in the preparative method, and especially temperature.

In *Figure 5* we compare the structure factors $S(Q)$ for a similar concentration range. The d-spacings corresponding to the observed peaks are listed in *Table 2* together with the particle dimensions where these were measured. *Figure 5* shows a transition from liquid-like to solid-like behaviour at around 4%, somewhat higher in concentration than the rheological measurements. However,the sensitivity of the particle size to temperature and therefore to sample preparation has already been noted. *Table 2* also shows that samples not in the sealed cells had smaller core radii and consequently smaller intermicelle spacing for fixed concentration (cf. equation (8)). The overlap concentration for the PEP sheath will tend to occur at lower concentrations for smaller micelles and this explains the differences observed in the transition region in *Figures 4* and *5* (in *Figure 6* we present SANS data from a 4% sample in a Couette cell. This sample clearly shows solid-like behaviour unlike the 4% sample in *Figure 4*).

Anisotropy (i.e. long-range organization) was generally observed for samples above 5% concentration.

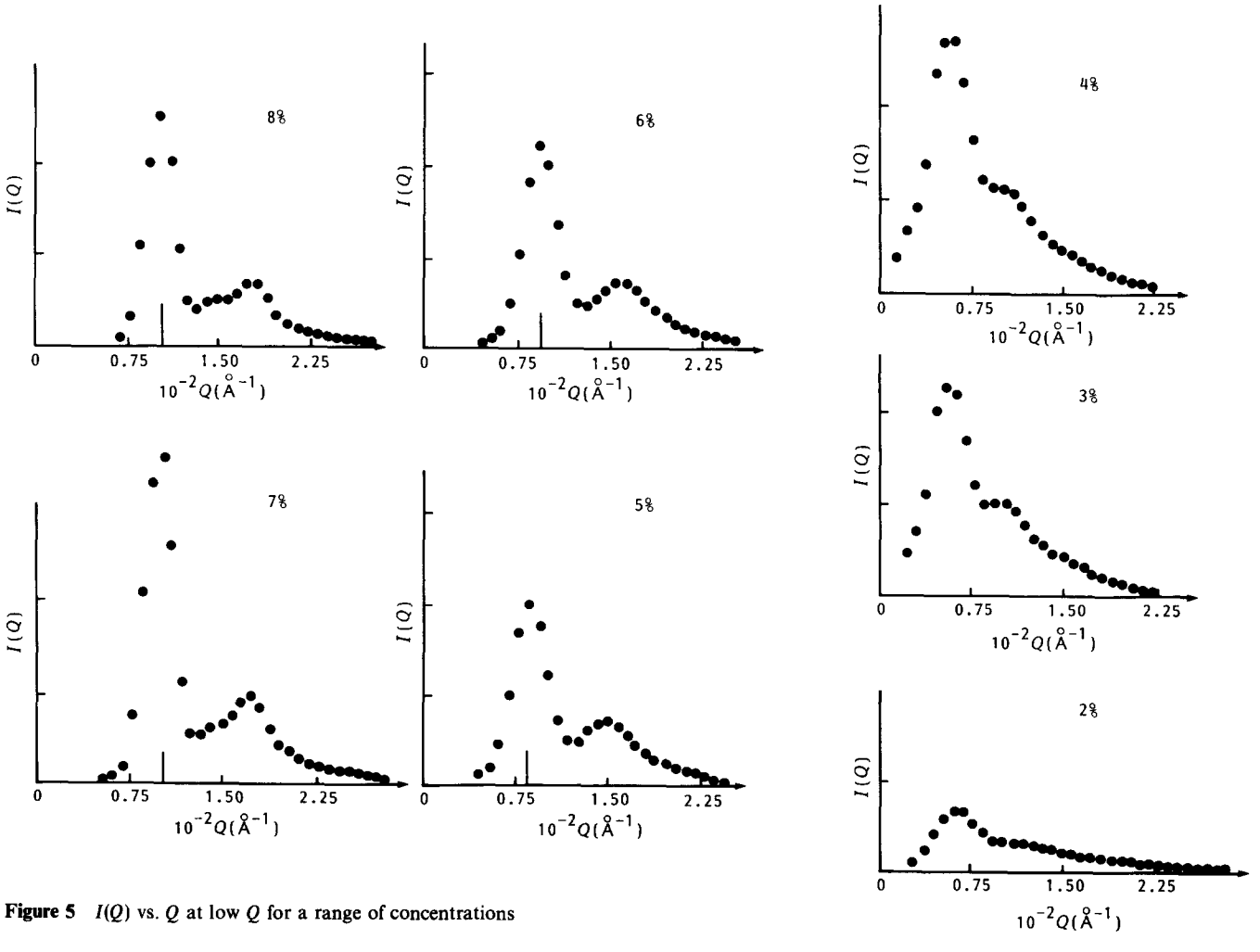

Figure 5 $I(Q)$ vs. Q at low Q for a range of concentrations

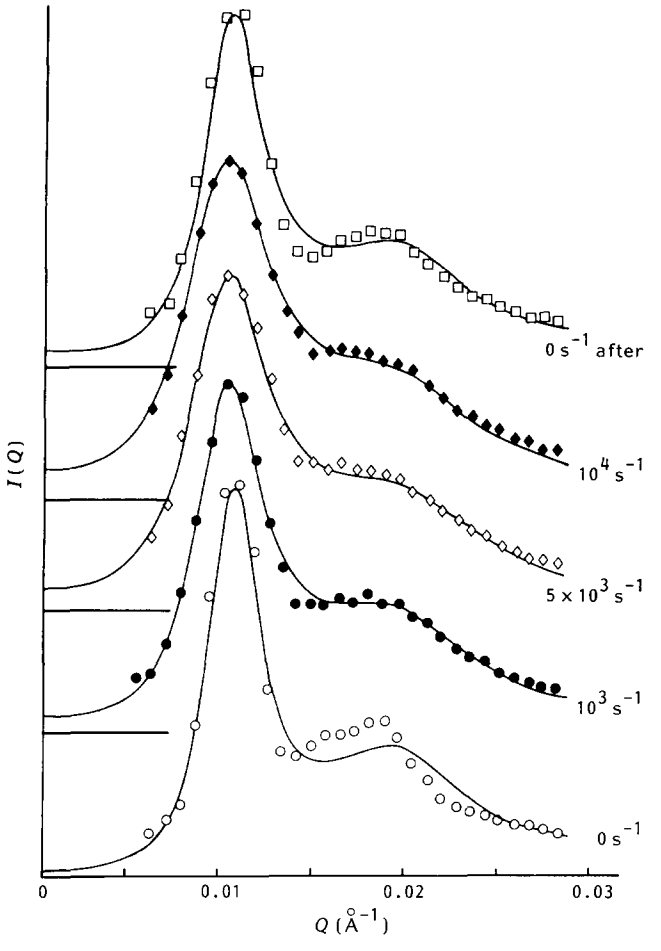

Figure 6 $I(Q)$ vs. Q for a 4% sample at low Q in a Couette cell at various shear rates as indicated

Both the rheological and the scattering data indicate that a structural change occurs at around 3 to 4% concentration. If we associate this with overlap of the PEP stabilizing sheath then *Table 2* allows us to estimate the extent of this sheath. By considering the interparticle spacing from $S(Q)$ and the particle radius from $P(Q)$ it is clear that order intervenes when the surface-to-surface spacing becomes less than about 450 Å. Thus the PEP sheath must extend at least 225 Å from the PS core if this sheath is responsible for the interparticle structure.

SANS experiments under shear and stress overshoot ratio

Figure 6 shows the effect of increasing shear rate in the Couette cell on the structure factor $S(Q)$ for a 4% sample. The maximum at low Q broadens but does not shift in Q and the secondary maxima at higher Q lose their structure and diminish in intensity. The final experiment at $0\ s^{-1}$ was carried out within 15 min of switching off the motor drive. Almost all the initial structure is recovered. This is consistent with the lack of hysteresis observed in the viscosity measurements. In *Figure 7*, however, we see that a small amount of initial vertical anisotropy—presumably introduced as the stator is lowered into the rotator and the sample forced upwards into the 0.5 mm spacing—is lost under shear and not recovered within this 15 min recovery time. This is consistent with the observations of the stress overshoot ratio shown in *Figure 8* for a 6% sample. This shows a monotonic increase in measured stress overshoot ratio when charted against the log of recovery time t. The behaviour is quite unlike that for normal polymer solutions of similar concentrations and coil overlaps, when ξ reaches a plateau at times of say $10–10^2$ s, but is very reminiscent of the behaviour of the weak gel system xanthan, whose non-linear viscoelastic behaviour has been studied by several groups[14]. The overshoot recovery experiment is a very testing probe of extremely long-range structure (i.e. macroscopic gel 'texture'), but its gradual increase implies that more short-ranged structure is rearranging itself during the time of the experiment.

Shear experiments were also carried out on an 8% sample. However, the high viscosity of this sample made it very difficult to load into the Couette cell. *Figure 9* shows that even at the beginning of the experiment there is rather less structure in $S(Q)$ than shown by a similar concentration sample in *Figure 5*. The two-dimensional plots showed no anisotropy. Presumably the long-range order was destroyed during the loading procedure and as shown in *Figure 8* has not had time to recover.

Model fits to the $I(Q)$ data

In *Figures 6* and *9* the full curves have been calculated from equations (1), (2) and (3) using the mean spherical approximation for charged suspensions developed by Hayter *et al.*[18–21]. $P(Q)$ is determined by the value chosen for R in equation (2), $S(Q)$ by the volume fraction η (or number density N) and by the form of the interparticle potential $U(r)$. In the model used $U(r)$ is a screened Coulombic form more normally associated with charge stabilized suspensions. It will be shown that the main features of this potential are, to a first approximation at least, easily transferable to a sterically based interaction. $U(r)$ is determined by the hard core diameter σ ($=2R$), the Debye screening length λ_D (or its inverse, κ) and the charge density q.

Then the potential is expressed as:

$$r<\sigma \quad U(r)=\infty \tag{9}$$

$$r>\sigma \quad U(r)=\frac{\pi\sigma^3 q^2}{4\varepsilon_0\varepsilon}\exp[-\kappa(r-\sigma)]/r$$

ε_0 is the permittivity of space and ε that of the sample.

In *Figure 10* the potentials used to calculate the curves in *Figure 6* are displayed. Each consists of a hard core region for $r<\sigma$ and a soft tail whose halfwidth is determined by κ^{-1}. When considering this potential in terms of the interactions between micelles in the present case, the hard core becomes the polystyrene core and the soft tail with its exponential decay is associated with the PEP sheath. In recent experiments on forces between surfaces bearing adsorbed polymer, Luckham and Ansarisar[22] have found force–distance profiles which also show a hard core and an approximately exponential decay. We thus interpret κ^{-1} as the range of the interaction between the PEP sheaths of the micelles and the charge density q as its strength.

In the program only two parameters are used for optimization. These are the hard core diameter σ and either the charge density q or the screening length κ^{-1}. The volume fraction η and the remaining potential parameter are chosen externally and fixed. Equation (8) shows that for fixed volume fraction η, σ and N are related

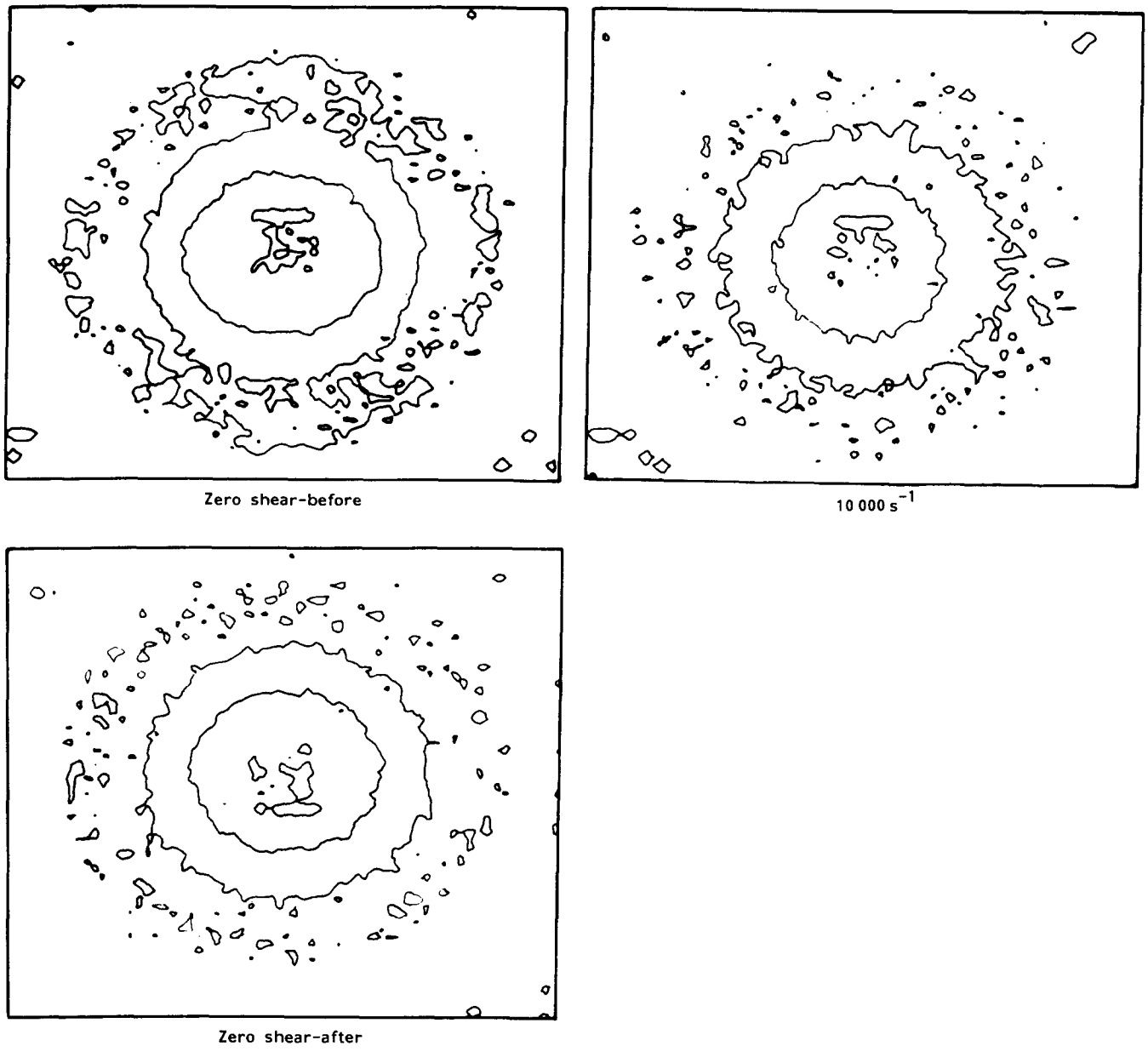

Figure 7 Two-dimensional intensity maps for some of the data in *Figure 6*

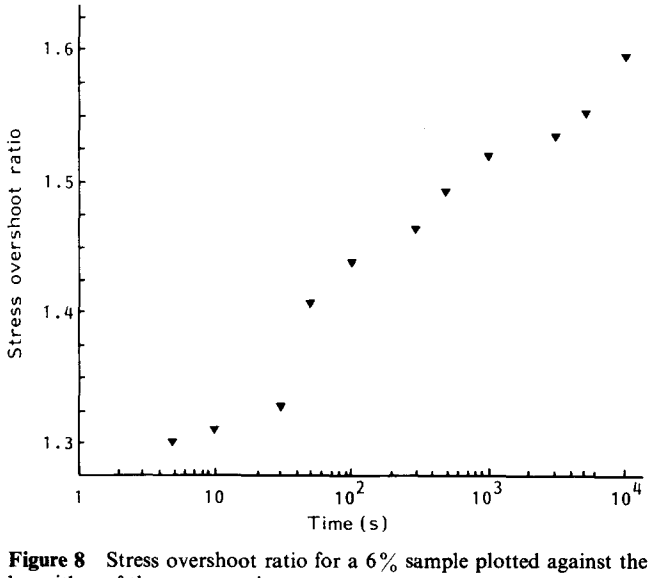

Figure 8 Stress overshoot ratio for a 6% sample plotted against the logarithm of the recovery time t

via

$$\eta = \pi N \sigma^{3/6}$$

In fitting the data in *Figures 6* and *9* we consistently found that the best fits were obtained only when the volume fraction was reduced below the values given by assuming all the polystyrene was in the micelle cores with a density of about 1.0 g cm^{-3}. Values of η were optimized for the zero-shear data and the best fits required a volume fraction of 0.023 and 0.011 for the 8% and 4% data respectively as compared to the values of 0.03 and 0.015 from *Table 3*.

The earlier arguments in the discussion of N and N' suggest that this discrepancy cannot be due to large quantities of copolymer in free solution, nor is a very high core density likely. We believe the discrepancy arises from the fact that the model assumes spherosymmetric structures while the data here are pseudo-lattice structures. The problem can be traced to the relationship between the number density N and $S(Q)$. For example, in

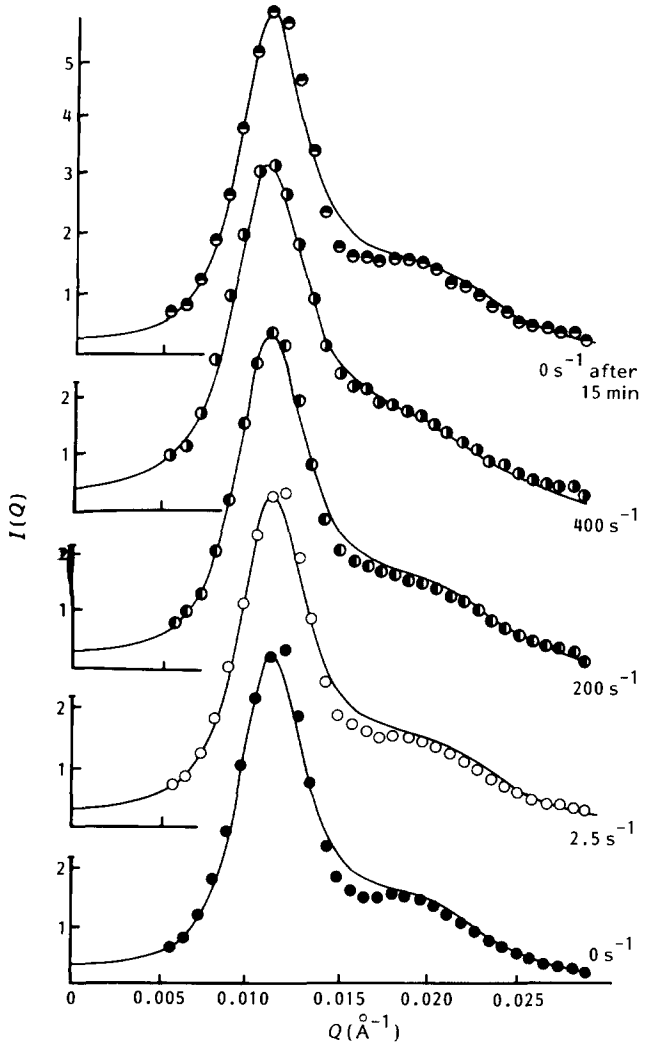

Figure 9 $I(Q)$ vs. Q for an 8% sample at low Q in a Couette cell at various shear rates as indicated

a simple cubic structure the first peak in $S(Q)$, $Q_{\max 1}$ is related to N by:

$$Q_{\max 1}/2\pi = N^{1/3} \tag{10}$$

whereas for body-centred cubic structures:

$$Q_{\max 1}/2\pi = 1.12N^{1/3} \tag{11}$$

The approximate relationship for the curves calculated in *Figures 6* and *9* is, however[13]:

$$Q_{\max 1}/2\pi = 1.18N^{1/3} \tag{12}$$

Thus this model requires an artificially low N to fit these data (for which N lies between b.c.c. and s.c. values) around $Q_{\max 1}$. If, however, the true value of η is given, then since $\eta = \pi N\sigma^{3/6}$ the program can only adjust N in order to fit the data around $Q_{\max 1}$ by altering σ and hence the shape of $P(Q)$ which has an adverse effect on the fit at high Q. In further support of this argument it was found that the values of σ obtained from these calculations agreed well with values of $2R$ obtained from the fitting $P(Q)$ alone (*Table 2*) only when the reduced volume fraction was used. Further comment on the values of σ will be made below.

Returning to *Figure 10* we can now examine the effect of the shear flow on the interparticle potential. All the fitted curves in *Figures 6* and *9* were obtained by fixing η and q at the optimum values for the zero-shear data and then allowing κ and σ to float. We were thus explicitly looking for changes in the range of the potential as shear increased. For both 4% and 8% data the fitted value of κ increased with increasing shear rate. The effect on the range of $U(r)$ for the 4% can be seen in *Figure 10*. There κ^{-1} decreases from 46.1 to 39.1 Å (i.e. the repulsion becomes more hard-sphere like) while σ remains almost constant at around 200 Å. The $P(Q)$ range was not observed directly for samples in the Couette cell, but the value of R for a similar sample in an unsealed cell is in good agreement at 96 Å. The very small changes observed

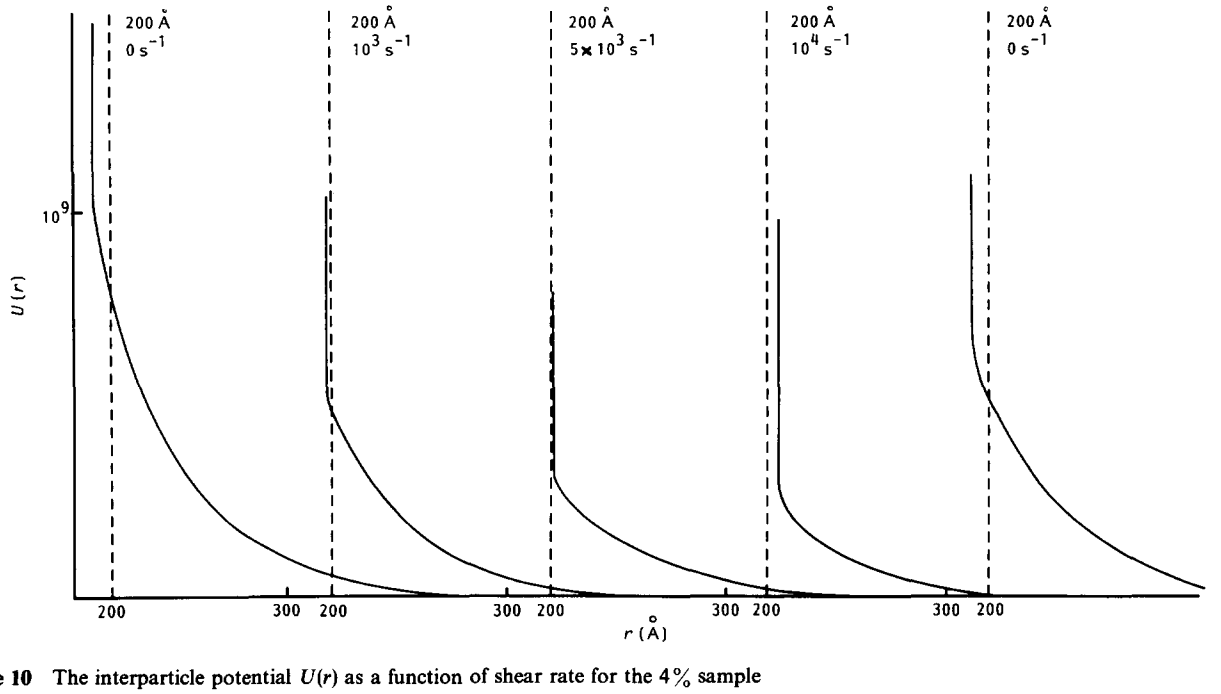

Figure 10 The interparticle potential $U(r)$ as a function of shear rate for the 4% sample

Table 4

w (wt%)	Temperature (K)	η	κ ($Å^{-1}$)	q	σ (Å)	$2R$ (from $P(Q)$) (Å)
2	300	00057	0.015	39.17	276	
3	300	0.0086	0.015	36.8	364	300±56
4	300	0.0114	0.015	19.26	385	
5	300	0.0142	0.02	49.21	257	260±84
6	300	0.0172	0.02	32.04	247	220±38
7	300	0.02	0.02	35.9	245	
8 (heated)	300	0.0229	0.02	15.06	198	184±26
9 (heated)	300	0.0258	0.02	12.3	206	200±50
10 (heated)	300	0.0287	0.02	10.9	201	214±32
8	300	0.0229	0.02	23.76	247	254±32
8	373↑	0.0229	0.02	22.0	230	
8	403	0.0229	0.02	14.96	193	
8	373↓	0.0229	0.02	15.1	196	
8	346	0.0229	0.02	10.3	200	
8	300	0.0229	0.02	15.06	198	184±26

in *Figure 10* are not, we believe, associated with true changes in $U(r)$ but rather with a change to more disordered structure which alters the relationship between $N^{1/3}$ and $Q_{\max 1}$ as in equations (10) to (12). *Figure 6* shows quite clearly the change in $S(Q)$ towards more disordered structure as the shear increases and it is notable that the fit to the data is much better at high shear as would be expected for a model based on random arrangement of particles.

As discussed previously the 8% data in *Figure 9* are already more 'disordered' at zero shear and the model is a correspondingly better fit. The value of κ^{-1} only changes slightly from 51.8 to 48.8 Å. The values of σ at around 230 Å are again in fairly good agreement with $R = 104$ Å for an 8% sample in an unsealed cell.

The correspondence between R and σ can be explored much more carefully for those cases where the $P(Q)$ and $S(Q)$ ranges were observed for the same sample.

Table 4 lists values of the parameters obtained by fitting the model to all the samples for which data in the $S(Q)$ range were available. Having decided as discussed above for the 4 and 8% samples under shear that a reduced value of η was appropriate we reduced all values of η by the same factor and then held them fixed. (In every case a cross check with a model fit using the experimental value of η ($= 0.38$ wt%/ρ) showed a markedly worsened fit.) As far as possible we fixed κ at the values previously found to give the best fit for the shear data and then explored the effect of temperature and concentration on q and σ. *Table 4* shows that a remarkably good agreement was found between σ and $2R$. It should be emphasized that these are fits of equations (1) to (3) to data obtained from the same sample in two different ranges of Q. In all cases the fits obtained were rather good close to $Q_{\max 1}$ but poor around the second peak in $S(Q)$ (as seen for the 4% data in *Figure 6*). This is almost certainly due to the inappropriateness of this model to the rather ordered structures. *Table 4* shows a number of further effects. The strength of the potential decreases with increasing concentration and with increasing temperature. Since, however, increasing temperature involves reduced σ and hence increased number density N it may be that in both cases increased number density means reduced intensity of the soft tail of the potential. One might say the particle repulsion becomes more hard-sphere like when they are forced closer together. Below 4% it was not possible to fit the data with the same value of κ as above this value, but with the reduced value (increased range) the intensity continues to rise as concentration is reduced.

CONCLUSIONS

In n-dodecane PS–PEP copolymer forms monodisperse micelles with polystyrene cores. These cores have radii between 100 and 150 Å depending on the exact thermal history of the samples. At concentrations above 3–4 wt% the micelles form ordered arrays which frequently show long-range anisotropy. These observations from SANS are in good agreement with rheological data, which show a change from liquid-like to soft solid-like behaviour over the same concentration range. At temperatures above 100°C dissociation begins to occur, with complete dissociation around 160°C. Samples at elevated temperatures form a larger number of smaller micelles when cooled. The equilibrium dimensions may be determined by surface-area requirements per molecule.

For a sample of 8% heated to 130°C (for which the particle radius changed from 127 Å before to 92 Å after heating, and the number density from 3.5×10^{15} to 9.2×10^{15}), the same preferred orientation was observed before and after heating. This observation is difficult to reconcile with a continuous three-dimensional array but might indicate the presence of sheets or rafts of ordered structure which become oriented on a microscopic scale.

The diffraction rings from the ordered structures are consistent with both simple cubic and body-centred cubic lattices. The calculated number densities also cannot discriminate unambiguously between these structures (the observed value lying between them) and thus may again indicate some alternative layered structure.

The observed ordered structure factors were fitted to a model calculated from a screened Coulombic potential (i.e. a hard core and a soft tail). The model parameters include the core diameter σ, which shows remarkably good agreement with values of R obtained from fitting the particle form factor $P(Q)$. The model calculations fit the data well around the first maximum of $S(Q)$ but not around the subsidiary maxima—presumably due to the inappropirateness of a liquid-like structure for these data. As shear rate increases the structure is apparently more disordered and the model fit improves. These changes appear in the model potential as increasingly hard-sphere like behaviour, i.e. the PEP sheath has less effect at higher shear rates. It is also found that the potential becomes more hard-sphere like as the interparticle spacing decreases.

Both SANS and rheological data agree that short-range order is quickly restored after flow stops but that long-range organization is very slow to reappear.

ACKNOWLEDGEMENTS

Dr S. Shakir prepared the micellar solutions and the authors would like to express their thanks. P.E.T. was supported by an SERC grant during this work. S.B. was a vacation student at Unilever, Colworth House, and would like to thank Mr R. Richardson and Mr H. McEvoy for support and encouragement. P.E.T. and J.S.H. would like to thank Dr A. Wright and Dr A. Rennie of the Institut Laue–Langevin for their assistance with the neutron experiments.

All the authors are grateful to Mrs Lesley Linger for her work in preparing the diagrams.

REFERENCES

1 Higgins, J. S., Dawkins, J. V., Maghami, G. G. and Shakir, S. A. *Polymer* 1986, **27**, 931
2 Price, C., Hudd, A. L., Stubbersfield, R. B. and Wright, B. *Polymer* 1980, **21**, 9
3 Price, C., Kendall, K. D., Stubbersfield, R. B., and Wright, B. *Polym. Commun.* 1983, **24**, 200, 326
4 Shibayama, M., Hashimoto, T. and Kawai, H. *Macromolecules* 1983, **16**, 16
5 Watanabe, H. and Kotaka, T. *Polym. Eng. Rev.* 1984, **4**, 1
6 Ibel, J. *J. Appl. Crystallogr.* 1976, **9**, 296
7 Lindner, P. and Oberthur, R. *Colloid Polym. Sci.* 1985, **263**, 443
8 Staples, E., Penfold, J. and Cummins, P. to be published (for details, E. Staples may be contacted)
9 Maconnachie, A. and Richards, R. W. *Polymer* 1978, **19**, 739
10 Jacrot, B. *Rep. Prog. Phys.* 1976, **39**, 311
11 Croxton, C. A. 'Introduction to Liquid State Physics', Wiley, New York, 1979
12 Riley, D. P. and Oster, G. *Faraday Disc. Chem. Soc.* 1951; **11**, 107
13 Brown, J. C., Pusey, P. N., Goodwin, J. W. and Ottewill, R. H. *J. Phys.* (*A*) 1975, **8**, 664
14 Richardson, R. K. and Ross-Murphy, S. B. *Int. J. Biol. Macromol.* 1987, **9**, 257
15 Candau, F., Heatley, F., Price, C. and Stubbersfield, R. B. *Eur. Polym. J.* 1984, **20**, 685
16 Mortensen, K., van Vlaak, K. and Schouten, M. private communication
17 Ferry, J. D. 'Viscoelastic Properties of Polymers', Wiley, New York, 3rd Edn, 1980
18 Bunce, J., Ramsay, J. D. F. and Penfold, J. *J. Chem. Soc. Faraday Trans. I* 1985, **81**, 2845
19 Penfold, J. and Ramsay, J. D. F. *J. Chem. Soc. Faraday Trans. I* 1984, **81**, 117
20 Hayter, J. B. and Penfold, J. *Mol. Phys.* 1981, **42**, 109
21 Hansen, J. P. and Hayter, J. B. *Mol. Phys.* 1982, **46**, 651
22 Luckham, P. F. and Ansarisar, N. A. *Polymer* 1988, **29**, 329